ELSEVIER

Energy and Buildings 34 (2002) 477–486

ENERGY and BUILDINGS

www.elsevier.com/locate/enbuild

Theoretical and computational analysis of closed wet cooling towers and its applications in cooling of buildings

Ala Hasan*, Kai Sirén

Helsinki University of Technology, Laboratory of Heating Ventilating and Air Conditioning, P.O. Box 4400, FIN-02015 Hut, Finland

Received 17 May 2001; accepted 2 November 2001

Abstract

Theoretical analysis and computational modelling of closed wet cooling towers (CWCTs) are presented. Experimental measurements for performance of a prototype tower are used to define the tower transfer coefficients. Tower flow rates and number of tubes and rows are optimised for the required cooling load and to achieve a high coefficient of performance (COP). The performance of a cooling system used to cool office buildings is simulated using the transient system (TRNSYS) simulation environment. The cooling system consisted of a CWCT, chilled ceilings, pumps and a fan. A control strategy, including night cooling, is introduced in the simulation. The results indicate efficient performance and high COP values for the system.

Keywords: Cooling tower; Chilled ceiling; Tower model; Simulation

1. Introduction

Chilled ceilings, having large surface areas, work according to the combined principles of radiation and convection heat transfer. They can work with low temperature differences between room air and the surface of the cooling panel. This results in lower air velocities in the room, so they can provide high level of indoor air comfort for the occupants. When compared with the conventional systems, the chilled ceilings require smaller volume for the distribution system, besides the ventilation rate can be reduced to lower levels. The use of water as the thermal carrier medium instead of air results in reduced energy demand for the pumping purpose. The use of relatively higher inlet cooling water temperatures, of about 20 °C, is possible which can be supplied by a closed wet cooling tower (CWCT).

Inside a CWCT, three fluids flow: cooling water, spray water and air. The cooling water is the fluid to be cooled, which flows inside tubes arranged in rows inside the tower. Spray water, injected on the tubes surfaces, re-circulates in a closed circuit, which makes it an intermediate fluid in the heat transfer process. Heat carried away from the building by the cooling water transfers to the spray water through the tube walls. From the spray water, it transfers to air by both sensible heat and latent heat. The latter makes the major contribution and is caused by the evaporation of a small amount of the spray water into the air stream. The use of the closed type of cooling towers, which is an indirect contact equipment, permits high level of cleanliness of the piping resulting in effective internal heat transfer surfaces, reduced maintenance costs and longer operational life.

A system consisted of a CWCT and chilled ceilings when used for cooling of buildings will result in a low cost, CFC free and environmentally clean system. The initial and running costs of the system are low when compared with traditional vapour-compression cooling systems. The low energy consumption results in higher coefficient of performance and lower CO_2 emissions. Fig. 1 shows the basic components of the cooling system. The CWCT, making use of the natural cooling effect, brings down the cooling water temperature to lower levels which depends on the outdoor air conditions and the effectiveness of the heat transfer process. The wet bulb temperature is, theoretically, the limit of the lowest temperature of an air–water contact operation with infinite surface area. The wet bulb temperature for many locations in Europe permits the use of this system. Fig. 2 shows the CWCT schematic.

By using a climate-dependent cooling system, overheating of a few days in the year is expected. It can be minimised by methods of utilisation of the stored cooling energy available during night, due to low wet bulb temperatures, which is also cheap due to low electric power expenses. These methods include the storage of cooling energy in the building mass by implementing a night cooling strategy [1] or the storage of cooled water in suitable tanks.

* Corresponding author. Tel.: +358-9-4513598; fax: +358-9-4513418.
E-mail address: ala.hasan@hut.fi (A. Hasan).

0378-7788/02/$ – see front matter
PII: S0378-7788(01)00131-1

Nomenclature

A	area (m^2)
C_H	specific heat capacity of moist air (kJ/(kg K))
C_W	specific heat capacity of water (kJ/(kg K))
COP	coefficient of performance
d	tube inside diameter (m)
D	tube outside diameter (m)
G_a	air mass velocity based on minimum section (kg/(s m^2))
h	enthalpy (kJ/kg)
h_{fg}	latent heat of evaporation of water (kJ/kg)
H	humidity ratio of moist air (kg water/kg dry air)
k	mass transfer coefficient (kg/(s m^2))
k_w	thermal conductivity of tube wall (W/(m K))
m	mass flow rate (kg/s)
N_r	number of rows
N_t	number of tubes
q	rate of heat transfer (W)
q_L	latent heat (W)
q_{sn}	sensible heat (W)
Re	Reynolds number
t	temperature (°C)
v_m	velocity of air in minimum section (m/s)
W	power consumption (W)

Greek letters

α	convective heat transfer coefficient (W/(m^2 K))
η	efficiency (fan or pump)
Γ	flow rate of spray water per unit breadth (kg/(s m))

Subscripts

a	air
c	cooling water
e	evaporation
i	interface
s	spray water
1	inlet to tower
2	outlet of tower

Superscript

$'$	saturated condition

CWCT are conventionally used for industrial applications in temperature ranges over that intended for the cooling of buildings. The designs for such purposes will result in overpowering in air flow and spray water flow when used for inlet cooling temperatures in the range of 23–25 °C.

A prototype of a counter-flow CWCT with a nominal cooling power of 10 kW was designed for cooling of office buildings. In this work, we will present the theoretical approach implemented to analyse the heat and mass transfer process in order to develop a computational model to simulate the operation of the CWCT. For a specific tower, it is necessary to correlate tower experimental data in order to determine the practical tower parameters. Therefore, the measurements from the prototype tower tests are used to conclude the tower transfer coefficients. The objective of achieving high coefficient of performance (COP) values and rejecting the required load calls for the optimisation of the tower flow rates and geometry in terms of air flow rate and relevant number of tubes and rows.

2. Literature review

Parker and Treybal [2] were the first researchers to present a detailed analysis of counter-flow evaporative liquid coolers based on four modes of operation of the cooler. The analysis assumed a linear function of air saturation enthalpy with temperature. Empirical correlations were presented for 19 mm o.d. staggered tubes. For the heat transfer coefficient (α_s) between tube wall and bulk of spray water

$$\alpha_s = 704(1.39 + 0.022t_s)\left(\frac{\Gamma}{D}\right)^{1/3} \tag{1}$$

where t_s is the spray water temperature, Γ the spray water flow rate per unit breadth and D the tube outside diameter. For the mass transfer coefficient (k) between the saturated air–water interface and the bulk air

$$k = 0.049G_a^{0.905} \tag{2}$$

where G_a is the air mass velocity.

Mizushina et al. [3] conducted series of tests on counter-flow evaporative coolers. Three coils having outside tube diameters of 12.7, 19.05 and 40 mm were used to find the effect of tube diameter on the heat and mass transfer coefficients. The results for the mass transfer coefficient were presented as a function of air Reynolds number (Re_a) and spray water Reynolds number (Re_s)

$$\alpha_s = 2100\left(\frac{\Gamma}{D}\right)^{1/3} \tag{3}$$

$$kA_V = 5.028 \times 10^{-8} Re_a^{0.9} Re_s^{0.15} D^{-2.6} \tag{4}$$

where A_V is the contact area per unit volume. These correlations are valid for the range of $1.5 \times 10^3 < Re_a < 8.0 \times 10^3$ and $50 < Re_s < 240$. It is apparent from Eq. (4) that Re_a is dominant.

In another paper, Mizushina et al. [4] set the design limitations for an evaporative liquid cooler taking into consideration the variation of spray water temperature inside the tower. The saturation enthalpy of air was considered as a linear equation over the operating temperature range and the evaporation of spray water was ignored.

Niitsu et al. [5–7] tested banks of plain and finned tubes. The plain tubes were 16 mm o.d. in a staggered arrangement. The correlations for plain tubes were

$$\alpha_s = 990\left(\frac{\Gamma}{D}\right)^{0.46} \tag{5}$$

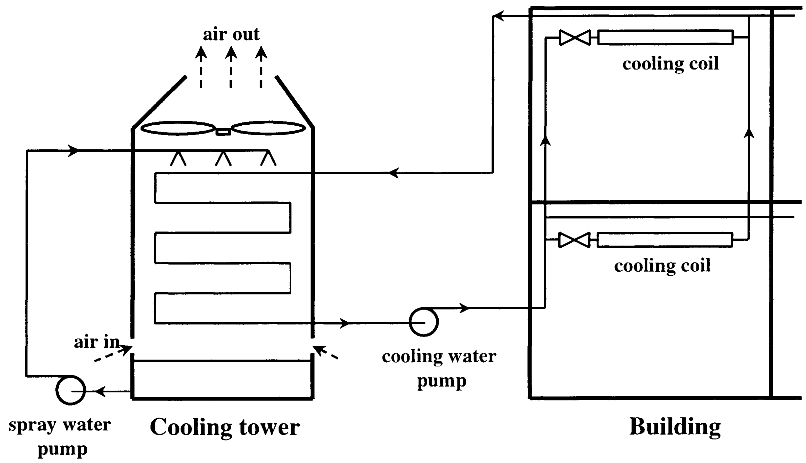

Fig. 1. System components.

$$k = 0.076G_a^{0.8}. \quad (6)$$

The presented correlations are in broad agreement. Finlay and Harris [8] mentioned that a single expression fitted to the correlations would show a scatter of perhaps ±30%, which is considered not excessive for a two-phase turbulent flow.

Koschenz [9] presented a model for CWCT to be used with chilled ceilings. He made two assumptions: first, constant spray water temperature along the tower and second that the spray water temperature was equal to the outlet cooling water temperature. However, spray water temperature is variable inside the tower and, if the heat loss from the spray water piping outside the CWCT casing is ignored, spray water temperature will be equal in the tower's inlet and outlet.

Zalewski and Gryglaszewski [10] presented a mathematical analytical model for the heat and mass transfer equations for evaporative fluid coolers. The analogy between heat and mass transfer was applied to find the mass transfer coefficient (k_x) from heat transfer correlations of fluid flow across tube bundles. The thickness of the spray water film was estimated and considered in the calculation of air velocity in the minimum flow section. A comparison was made with experimental results of an evaporative cooler made from steel tubes having 25 mm o.d. in a staggered arrangement of 14 tubes comprising four rows. A correction for the mass transfer coefficient was suggested as a function of inlet air wet bulb temperature t_{wb} to improve the agreement between the experimental and the calculated data as follows

$$k = 2.937\exp(-0.0834t_{wb})k_x. \quad (7)$$

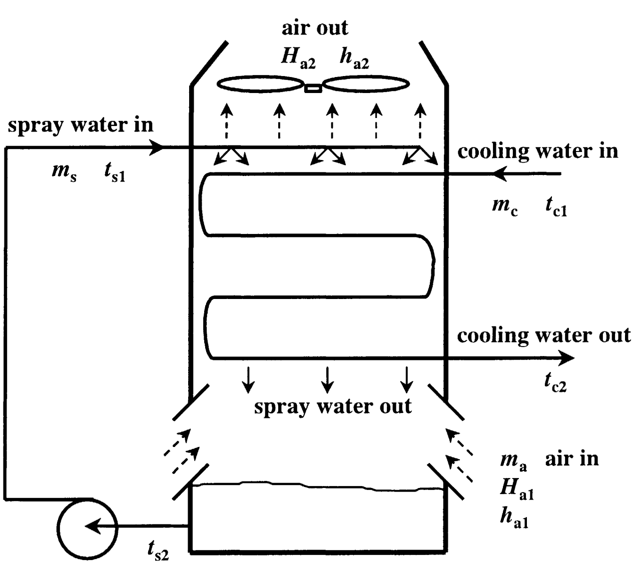

Fig. 2. Tower arrangement.

Gan and Riffat [11] applied computational fluid dynamics (CFD) to predict the performance of a CWCT as applied to the two-phase flow of air and water droplets, assuming uniform volumetric heat flux distribution in the tube coils. The computational results showed an increase of cooling water temperature for the lower tube rows in the tower. This behaviour was attributed to the assumption of uniform heat flux generation. In reality, heat flux is higher for the upper rows because of the higher inlet cooling water temperatures. In a recent paper, Gan et al. [12] assumed a linear heat flux distribution along the tower, which was twice as high for the upper rows as for the bottom rows. In a conclusion of the analysis for the pressure field, the predicted pressure losses for a single-phase flow of air over the tubes were in good agreement with estimated values from empirical equations. For the thermal performance of the tower, it was concluded that it is essential to incorporate models for the thermal performance of the tower to be used with CFD to define the heat flux distribution; otherwise any assumed heat flux distribution will yield inaccurate results.

3. Theoretical analysis

For a steady-state condition, it is assumed that the spray water flow rate is sufficient to wet all the surfaces of the

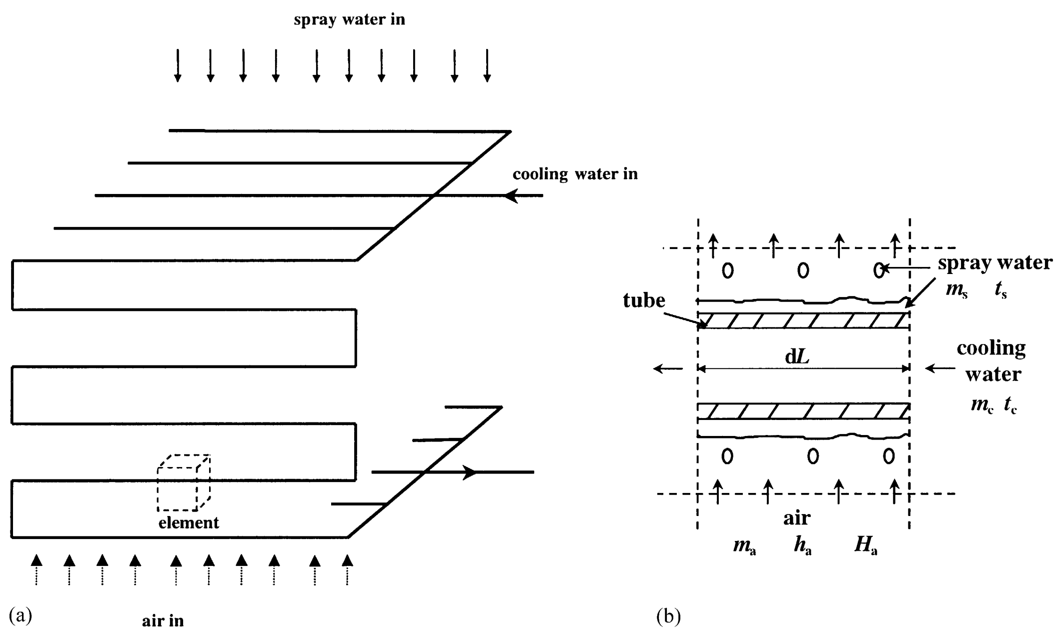

Fig. 3. Flow streams: (a) around tube coils; (b) inside an element.

tubes. Fig. 3a shows the tube coils inside the tower. Taking an element of tube area of dA, Fig. 3b shows the direction of the flow of the three streams (cooling water, spray water and air) inside the element. The analysis of the energy and mass balance for the tube element will define the mathematical equations for the tower performance.

3.1. Energy balance

3.1.1. Heat transfer from cooling water to spray water

The heat load of the building is carried away by the cooling water, which results in its temperature increase. In the tower, and as a result of the temperature gradient between cooling water temperature (t_c) and spray water temperature (t_s), heat transfers through the tube wall to the spray water. The rate of heat lost by the cooling water (dq_c) is

$$\mathrm{d}q_c = m_c C_W \,\mathrm{d}t_c = -U_o(t_c - t_s)\,\mathrm{d}A \tag{8}$$

where U_o is the overall heat transfer coefficient based on the outer area of the tube. It accounts for the heat transfer coefficient between the cooling water and the internal surface of the wall (α_c), the tube wall thermal conductivity (k_w) and the heat transfer coefficient between the external surface of the wall and the spray water bulk (α_s). It can be written as

$$\frac{1}{U_o} = \frac{1}{\alpha_c}\left(\frac{D}{d}\right) + \frac{D}{2k_w}\ln\left(\frac{D}{d}\right) + \frac{1}{\alpha_s} \tag{9}$$

where D and d are the outside and inside tube diameters, respectively.

3.1.2. Heat transfer from air–water interface to air bulk

Heat gained by air stream (dq_a) is due to heat transferred from the air–water interface. It consists of sensible part (dq_{sn}) and latent part (dq_L)

$$\mathrm{d}q_a = m_a\,\mathrm{d}h_a = \mathrm{d}q_{sn} + \mathrm{d}q_L. \tag{10}$$

Substituting for the sensible and latent heats gives

$$\mathrm{d}q_a = m_a\,\mathrm{d}h_a = \alpha_i(t_i - t_a)\,\mathrm{d}A + k(H_i' - H_a)h_{fg}\,\mathrm{d}A \tag{11}$$

where α_i is the heat transfer coefficient for the air side of the interface, h_{fg} the latent heat of evaporation of water and H_i' the humidity ratio of saturated moist air at the interface temperature (t_i).

The enthalpy of air and water vapour mixtures is represented by

$$h_a = C_H t_a + h_{fg} H_a \tag{12}$$

where C_H is the specific heat capacity of humid air which could be considered constant. Thus, the temperature of moist air can be written as

$$t_a = \frac{h_a - h_{fg} H_a}{C_H} \tag{13}$$

Substituting for t_a and t_i from Eq. (13) in Eq. (11) yields

$$m_a\mathrm{d}h_a = \left\{\alpha_i\left[\frac{(h_i' - h_{fg}H_i')}{C_H} - \frac{(h_a - h_{fg}H_a)}{C_H}\right] + k(H_i' - H_a)h_{fg}\right\}\mathrm{d}A. \tag{14}$$

Hence,

$$m_a\,\mathrm{d}h_a = \left[\frac{\alpha_i}{C_H}(h_i' - h_a) + h_{fg}k\left(1 - \frac{\alpha_i}{kC_H}\right)(H_i' - H_a)\right]\mathrm{d}A. \tag{15}$$

The term α_i/kC_H appearing on the right hand side of Eq. (15) is called the Lewis relation. The Lewis number (Le) is defined as

$$Le^{1-n} = \frac{\alpha_i}{kC_H}. \tag{16}$$

It expresses the relative rates of propagation of energy and mass inside a system. According to ASHRAE Fundamentals [13] for air and water vapour mixtures the Lewis relation could be taken as

$$\frac{\alpha_i}{kC_H} \approx 1. \tag{17}$$

Hence, Eq. (15) is reduced to

$$m_a\,dh_a = k(h'_i - h_a)\,dA. \tag{18}$$

The liquid side of the interface offers a negligible resistance to heat transfer [14], so that the interface enthalpy (h'_i) in Eq. (18) could be considered equal to the saturated air enthalpy (h'_s) at the spray water temperature (t_s). Therefore, Eq. (18) is rewritten as

$$dq_a = m_a\,dh_a = k(h'_s - h_a)\,dA. \tag{19}$$

Eq. (19) is called the Merkel equation [15]. It shows that the energy transfer could be represented by an overall process based on enthalpy potential difference, between air–water interface and bulk air, as the driving force.

3.1.3. Total energy balance for the element

The energy balance for the three streams flowing inside the element shown by Fig. 3b gives

$$dq_c + dq_a + dq_s = 0. \tag{20}$$

The spray water heat transfer dq_s can be represented by

$$dq_s = C_W\,d(m_s t_s) \tag{21}$$

where m_s is the spray water mass flow rate. It is a usual practice to assume m_s constant in Eq. (21) [14]. This can be explained, for example, by assuming the total rejected heat as latent heat only, dq_L in Eq. (10), which will give maximum variation of m_s due to evaporation. Therefore, for 10 kW power, the evaporation rate will be less than 0.3% of the nominal spray water flow rate of 1.37 kg/s, which confirms the assumption of constant m_s in Eq. (21). Hence, Eq. (20) becomes

$$m_c C_W\,dt_c + m_a\,dh_a + m_s C_W\,dt_s = 0. \tag{22}$$

3.1.4. Spray water temperature distribution

Spray water temperature varies inside the tower according to the height of the element. If the spray water piping outside the tower is assumed insulated or practically the heat loss is negligible, the inlet spray water temperature will equal the outlet spray water temperature

$$t_{s1} = t_{s2}. \tag{23}$$

The term dq_s will disappear from Eq. (20) when applied to the whole tower.

For the upper rows, as a result of the high inlet water temperature and the high air enthalpy, which has been raised through air flow inside the tower, part of the heat lost by cooling water is retained in the spray water resulting in the increase of t_s. For the lower rows, the inlet air enthalpy is low, the spray water losses its heat to air at an increased rate resulting in the decrease of t_s. This phenomenon regulates the spray water temperature distribution along the tower height.

3.2. Mass balance

To calculate the rate of spray water evaporation (m_e), the mass balance for the element gives

$$m_e = m_a\,dH_a = k(H'_s - H_a)\,dA. \tag{24}$$

Eqs. (8), (19) and (22)–(24) govern the heat and mass transfer process for the elements in the tower.

4. Computational model

4.1. Model solution procedure

The tower is divided into elementary volumes, each surrounding a tube of length dL and area dA, as shown in Fig. 3b. On the surface boundaries, the properties of cooling water, spray water and air are defined.The calculation of the energy and mass balance is carried out for each element. The exchanged data between the adjacent elements depend on the direction of the flow: horizontally for the cooling water temperature and vertically for the spray water temperature (downward) and the air properties (upward). For specified mass flow rates and transfer coefficients (k and α_s), the number of variables included in the heat and mass transfer equations for each element is eight: the inlet and outlet values of t_c, t_s, h_a and H_a. The input parameters for the tower are three (t_{c1}, h_{a1} and H_{a1}) and the balance equations are five (Eqs. (8), (19) and (22)–(24)), which will render the solution applicable.

The solution starts by taking the first element uptower, surrounding the cooling water inlet tube and proceeds in the direction of the cooling water flow. The scattering of the tower inlet parameters uptower (for the inlet cooling water t_{c1}) and downtower (for the inlet air state h_{a1} and H_{a1}) calls for the implementation of iterative methods. This is achieved by guessing values for h_{a2} and t_{s1} in the uptower section. The first values are the inlet air wet bulb temperature for t_{s1} and the outdoor air enthalpy for h_{a2}.

First, iterations are carried out to approach the equality of t_{s1} and t_{s2} (Eq. (23)). Subsequently, another iteration is executed to check the computed inlet air enthalpy with the inlet air state h_{a1}. The latter iteration will alter the solved value for t_{s1}, therefore, successive iterations are needed for the two solutions which will lead, eventually, to the convergence of the solution.

The design data for a 174.654 kW evaporative liquid cooler mentioned by Mizushina et al. [4] is fed to the model. The cooler consists of 20 tubes of 34 mm o.d. arranged in 13 rows, the inlet temperature is 50 °C. It is noted that a

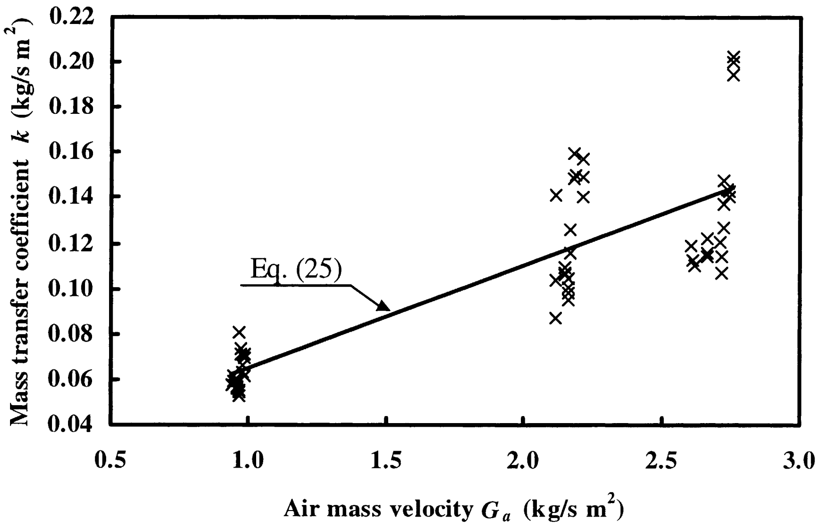

Fig. 4. The mass transfer coefficients computed from the experimental measurements and the concluded mass correlation equation.

difference of less than 1% exists between model output and the design data for the power estimation, which confirms the accuracy of the model.

This model is used to simulate the operation of the CWCT prototype in the cooling system. The simulation of the cooling system will be presented in a later section.

4.2. Tower transfer coefficients

The prototype tower consists of 19 tubes of 10 mm o.d. arranged in 12 rows in a staggered arrangement with a tower width of 0.6 m. Each tube has a 1.2 m length in one row. The longitudinal and transversal spacing of the tubes are 0.02 and 0.06 m, respectively. Nominal data for the tower are: 3.0 kg/s air flow rate, 0.8 kg/s cooling water flow rate, 1.37 kg/s spray water flow rate, inlet cooling water temperature of 21 °C and inlet wet bulb temperature of 16 °C.

The tower prototype was installed in Porto. The project partner (Faculty of Engineering at the University of Porto) supplied the measurement data obtained from the tower tests, which showed that the spray water temperature at the tower inlet was lower than that at the tower sump by approximately 0.3 °C. This difference could be due to the fact that the tower sump tank and the spray water piping outside the tower were not insulated, which is a practical case.

We can assume that the theoretical analysis of the closed wet tower is fulfilled and the total heat rejected by the cooling water is transferred to the air stream (i.e. no heat is lost from the tower casing and piping). For such a case and for each set of test data, the mass flow rates, inlet air state and inlet cooling water temperature supplied by the test measurements are fed to the model as input data. Therefore, the inlet and outlet spray water temperature can be computed as a unique value. When the measured outlet cooling water temperature (t_{c2}) is given as input data to the model, the unknown will be the mass transfer coefficient of the tower (k), whereas, the Parker and Treybal correlation, Eq. (1), is used to estimate the heat transfer coefficient (α_s).

The parameter influencing the value of k is the Re_a. Therefore, for the specific geometry of the tower, the correlation equation for the mass transfer coefficient could be presented as a function of the air mass velocity (G_a), which is based on the air velocity in the minimum section v_m. The correlation concluded for a total of 60 sets of measurements for $0.96 < G_a < 2.76$ kg/(s m^2) is

$$k = 0.065 G_a^{0.773}. \tag{25}$$

Fig. 4 shows the scatter of the mass transfer coefficients computed from the test data and the concluded correlation equation. Model outputs using this correlation show good estimation of the rejected heat. For 57 test sets, the ratio of the computed to the experimental rejected heat is between 92 and 115%, as shown by Fig. 5. The concluded correlation

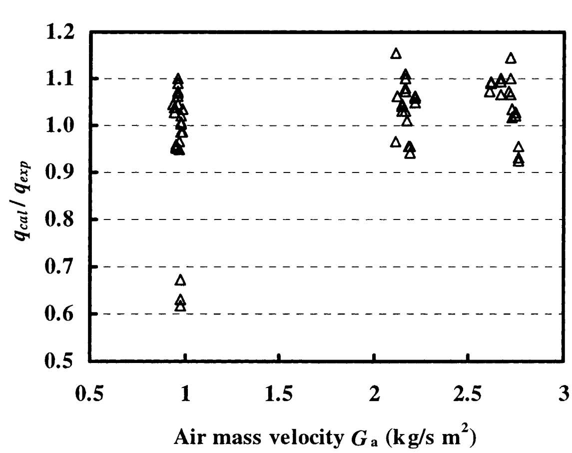

Fig. 5. The ratio of the calculated heat transfer rate by the model (q_{cal}) to the heat transfer rate from the experimental measurements (q_{exp}).

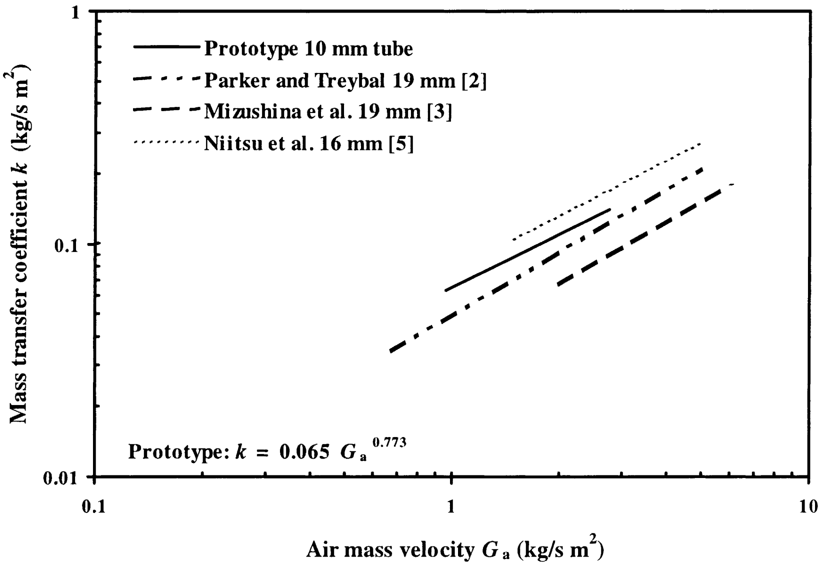

Fig. 6. Comparison of prototype tower mass transfer coefficients with other works.

is shown in Fig. 6 on a logarithmic scale as compared with correlations for other work conducted by Parker and Treybal [2], Mizushina et al. [3], and Niitsu et al. [5–7]. Fig. 6 shows that Eq. (25) falls within the range of the similar correlations.

The transfer coefficients of the tower should be independent of the cooling water temperature because it is included in the physical analysis. Therefore, the effect of the inlet cooling water temperature on the tower coefficient is not considered, a conclusion similarly arrived at by Facão and Oliveira [16], according to their experimental observations.

4.3. Model outputs

Establishing the tower transfer coefficients and using the presented model, it is possible to predict the performance of the tower with variable flow rates and outdoor air conditions. The experimental data did not include the nominal air flow of 3.0 kg/s as a result of technical difficulties concerning the capacity of the fan. However, it is possible to predict the tower performance for the nominal air flow rate, for which Fig. 7 shows the temperature and enthalpy distributions for the mid-row elements along the tower. Row height 12 refers to the highest row elevation. Fig. 7a shows cooling water temperature decrease, air dry bulb temperature decrease and spray water temperature distribution. This last increases for the upper rows and decreases for the lower rows. The inlet air dry bulb temperature is assumed to be 20 °C and as it appears from Fig. 7a that air dry bulb temperature is higher than spray water temperature, the direction of sensible heat transfer is from air to spray water. The result is air dry bulb temperature decrease. This means that air loses heat as sensible heat, but simultaneously gains heat as latent heat which is associated with the increase in its moisture content due to water evaporation. The latent heat rate is higher, which results in the increase of air enthalpy, as shown by Fig. 7b.

Fig. 8 shows the distribution of the rejected heat per row for one tube along the tower. As is shown, heat distribution has an exponential form. This explains inaccuracies encoun-

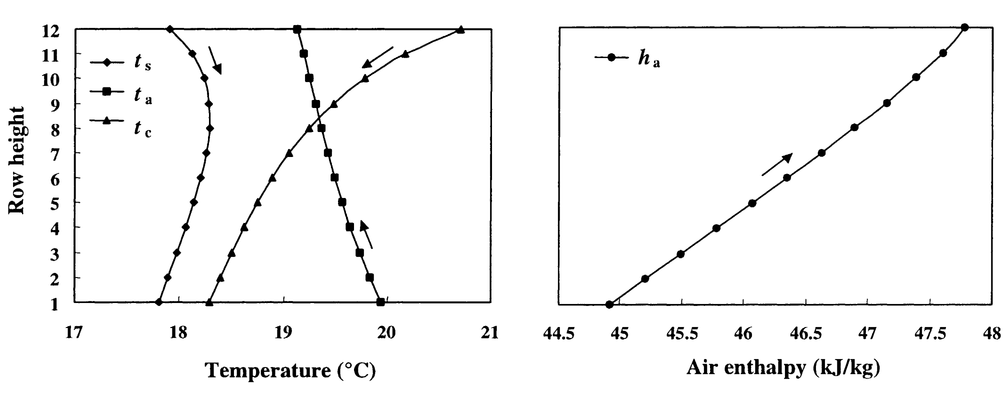

Fig. 7. Predicted temperature distribution (t_s, t_a and t_c) and air enthalpy distribution (h_a) along the tower for the nominal conditions.

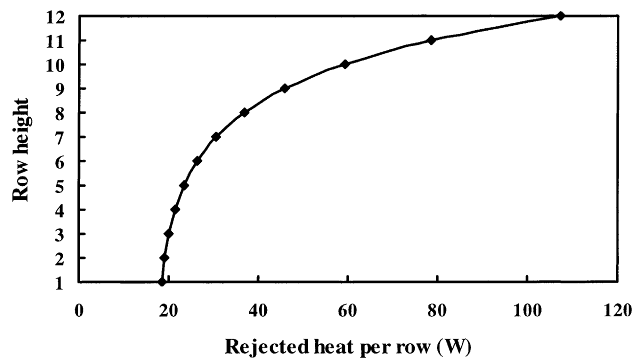

Fig. 8. Model output for the variation of the rejected heat per row for one tube along the tower for nominal conditions and tower geometry.

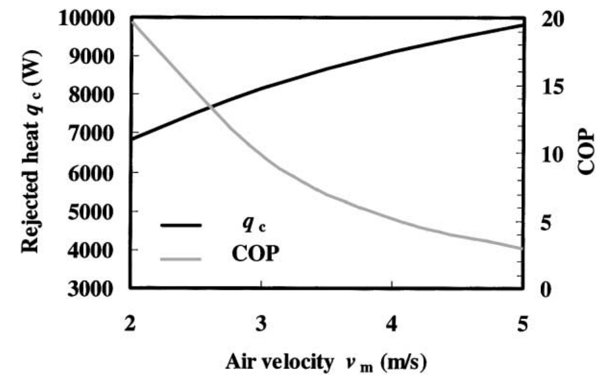

Fig. 9. Effect of air velocity on the tower rejected heat and COP for nominal tower geometry ($N_t = 19$ and $N_r = 12$).

tered in calculations when assuming a uniform or a linear heat flux distribution.

5. Optimisation of flow rates and number of tubes and rows

Model output shows that, for the nominal tower data, the rejected heat (q_c) is 9250 W and the COP is 4.6. The COP defined as

$$\mathrm{COP} = \frac{q_c}{W_{tot}}. \tag{26}$$

W_{tot} is the total power consumption defined as

$$W_{tot} = W_f + W_s \tag{27}$$

where W_f is the fan power and W_s is the spray water pump power. The predicted total power consumption for the nominal case is 1990 W from which the fan takes the major share, 1850 W.

5.1. Effect of air velocity on rejected heat and COP

The analysis of the total power consumption would give it as a function of the following variables

$$W_{tot} = f(N_t, N_r, v_m, \eta_f, \eta_s) \tag{28}$$

where N_t and N_r are the number of tubes and rows, respectively and v_m the air velocity in the minimum section. The fan and pump efficiencies (η_f, η_s) can be found from manufacturer's data. Therefore, for a specific geometry, Eq. (28) will be a function of v_m alone. In Fig. 9, the tower performance parameters (q_c and COP) are shown as determined by v_m for the nominal number of tubes and rows. The air velocity v_m is 4.1 m/s for the nominal air flow rate. From this figure, it appears that as v_m increases, the rejected heat (q_c) increases; the disadvantage is low COP values. The nominal cooling power of 10 kW will be possible with higher air velocities which means low COP for the system, therefore, the tower geometry and air flow rate should be reviewed for better performance.

Assuming that the longitudinal and transversal tube spacing is maintained similar to that of the tower prototype, a study of the optimum overall tower geometry in terms of number of rows and tubes, and air and spray water flow rates is possible to satisfy high tower performance parameters (q_c and COP). This can be achieved by considering the pressure drop data from the test measurements that are used to estimate the pressure drop for various air and water velocities. The concluded correlation equation (Eq. (25)), can be used to find the mass transfer coefficient as a function of air velocity. Therefore, the number of rows and tubes can be optimised for the tower performance as a function of air velocity.

5.2. Effect of increase of number of tubes and rows

For a constant air velocity, when the number of tubes (N_t) and number of rows (N_r) increase, the contact area will increase which will result in increased rejected heat as shown by Fig. 10. This will cause a decrease in COP due to higher relative power requirements coming from higher air flow rate and related increased pressure drop as shown by Fig. 11. However, the power requirements for a large tower with a low air velocity are lower when compared with a small tower with a high air velocity because the total power

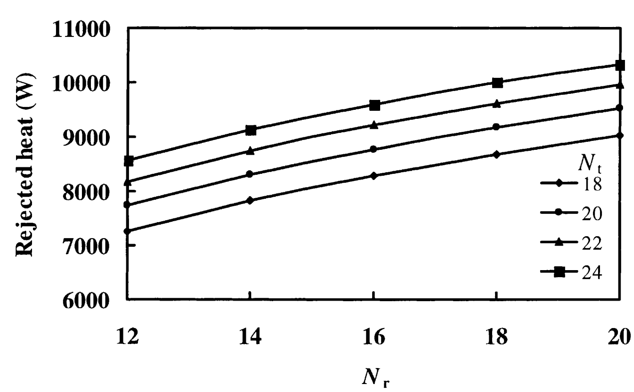

Fig. 10. The effect of variation of the number of tubes (N_t) and number of rows (N_r) on the tower rejected heat for 2.4 m/s air velocity in the minimum section.

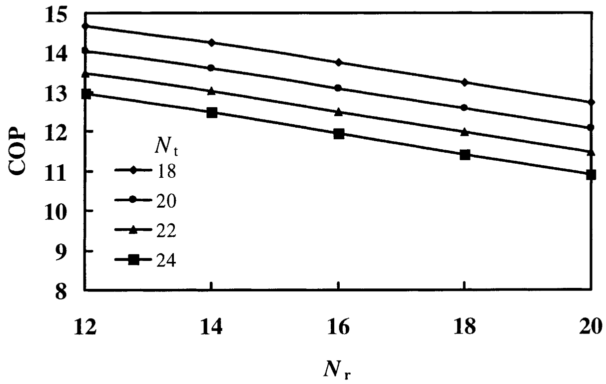

Fig. 11. The effect of variation of the number of tubes (N_t) and number of rows (N_r) on the system COP for 2.4 m/s air velocity in the minimum section.

requirements are proportional to v_m^3. Therefore, better performance coefficient could be obtained when operating with low air velocity and high contact area. An optimum selection of N_t and N_r is possible from Figs. 10 and 11.

From these two figures, it appears that rejected heat of 10 kW and a COP value of 11.4 could be obtained when $N_r = 18$ and $N_t = 24$. In this case: $m_a = 2.23$ kg/s, $m_s = 1.73$ kg/s and $W_{tot} = 875$ W from which 700 W is the fan power.

This analysis is carried out for the nominal operating conditions, the actual operating conditions are climate dependent, location and season. However, the improved performance for the reference nominal operating conditions will give indications of improved performance for the actual operating conditions.

6. Cooling system simulation

The performance of the entire cooling system presented in Fig. 1 is simulated by integrating the CWCT model, chilled ceilings model and building model using the transient system (TRNSYS) simulation environment [17]. The control strategy for the efficient operation of the system, including a night cooling strategy, is also considered in the system simulation.

An office building is assumed with room dimensions of 2.9 m height, 9.7 m^2 floor area and having two windows each of 1.26 m^2 area. The rooms are assumed located in two opposite orientations (north and south) to give variable cooling loads simultaneously. It is assumed that one occupant exists in the room which contains a computer, a printer and lighting, used for 8 h on working days.

A simple night cooling control is adapted. A linear set-temperature variation for the time between 18:00–24:00 and 00:00–08:00 h is suggested, with a minimum set temperature of 15 °C at 24:00 h. The cooling panel area is assumed 6.6 m^2 based on medium value for office applications.

The optimised numbers of tubes and rows are considered for the CWCT in the simulations. A criterion is applied that

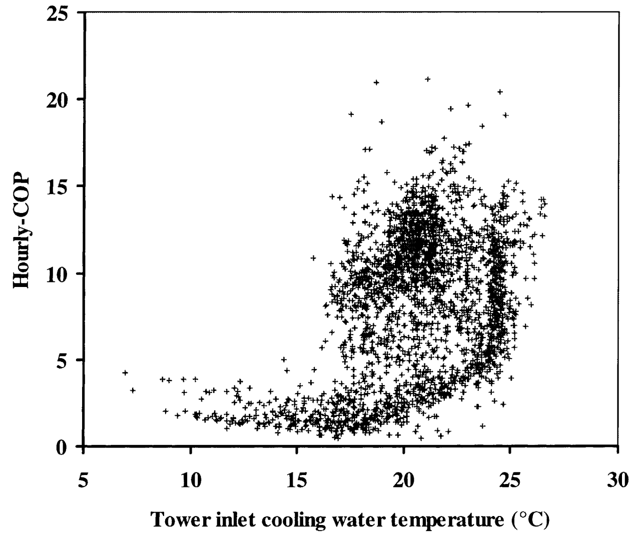

Fig. 12. System simulation output: the hourly-COP values for a building in Zurich (1 April–31 October).

limits a total annual maximum time of 40 h for room temperatures higher than 26 °C. The building area is chosen to satisfy this criterion. The simulation is carried out using the climatic test reference year files for four locations in Europe: Helsinki, Lisbon, London and Zurich. The results of the simulation show that the yearly COPs are higher than the COPs for conventional vapour compression systems. For example, for an office building in Zurich with a total floor area of 563 m^2 (58 rooms), the system COP would be 8.4 for the period from 1 April to 31 October. Fig. 12 shows the system hourly-COP versus the tower inlet cooling water temperature.

7. Conclusions

A computational model is developed based on the theoretical analysis of the performance of a CWCT. The transfer coefficients of the tower are concluded from test measurements of the thermal performance of the tower prototype. The measurement data for the pressure drop and the transfer coefficients are used to optimise the number of tubes and rows and the tower flow rates in order to achieve the nominal rejected heat and high COP values.

The cooling system consists of a 10 kW nominal power CWCT and chilled ceilings. The model developed for the CWCT is integrated into a global system simulation program that includes the transient building simulation model, chilled ceiling model, night cooling strategy, system control and models for other components. The implementation of CWCTs in cooling of buildings shows efficient performance with high COP values. The results of the simulation indicate acceptable indoor air temperatures and relatively high COP for four locations in Europe, Helsinki, Lisbon, London and Zurich. The simulation results for an office building in Zurich show a COP of 8.4. The system primary and operating costs are low and it is environmentally clean.

Acknowledgements

The partners of the ECOCOOL project are greatly acknowledged: Sulzer Infra Lab (CH), Sulzer Escher Wyss Lindau (DE), University of Porto (PO) Faculty of Engineering, University of Nottingham (UK) Institute of Building Technology. The work is partially funded by the Commission of the European Union (DGXII), Joule IV programme.

References

[1] P. Sprecher, B. Gasser, O. Böck, P. Kofoed, Control strategy for cooled ceiling panels, ASHRAE Transactions 101 (2) (1995)711–716.

[2] R.O. Parker, R.E. Treybal, The heat mass transfer characteristics of evaporative coolers, Chemical Engineering Progress Symposium Series 57 (32) (1962).

[3] T. Mizushina, R. Ito, H. Miyashita, Experimental study of an evaporative cooler, International Chemical Engineering 7 (4) (1967).

[4] T. Mizushina, R. Ito, H. Miyashita, Characteristics and methods of thermal design of evaporative cooler, International Chemical Engineering 8 (3) (1968).

[5] Y. Niitsu, K. Naito, T. Anzai, Studies on characteristics and design procedure of evaporative coolers, Journal of SHASE, Japan 41 (12) (1967).

[6] Y. Niitsu, K. Naito, T. Anzai, Studies on characteristics and design procedure of evaporative coolers, Journal of SHASE, Japan 41 (13) (1967).

[7] Y. Niitsu, K. Naito, T. Anzai, Studies on characteristics and design procedure of evaporative coolers, Journal of SHASE, Japan 43 (7) (1969).

[8] I.C. Finlay, D. Harris, Evaporative cooling of tube banks, International Journal of Refrigeration 7 (4) (1984).

[9] M. Koschenz, Model for closed circuit evaporative cooling tower, in: Proceedings of the 4th International Conference of IBPSA International Building Performance Simulation Association, Madison, WI, USA, August 1995.

[10] W. Zalewski, P.A. Gryglaszewski, Mathematical model of heat and mass transfer processes in evaporative fluid coolers, Chemical Engineering and Processing 36 (1997)271–280.

[11] G. Gan, S.B. Riffat, Numerical simulation of closed wet cooling towers for chilled ceiling systems, Applied Thermal Engineering 19 (12) (1999).

[12] G. Gan, S.B. Riffat, L. Shao, P. Doherty, Application of CFD to closed wet cooling towers, Applied Thermal Engineering 21 (1) (2001).

[13] ASHRAE Fundamentals, American Society of Heating, Refrigeration and Air Conditioning Engineers, USA, 1997.

[14] ASHRAE Systems and Equipment, American Society of Heating, Refrigeration and Air Conditioning Engineers, USA, 1992.

[15] F. Merkel, Verdunstungskuehlung, VDI Forschungsarbeiten No. 275, Berlin, 1925.

[16] J. Facão, A. C. Oliveira, Thermal behaviour of closed wet cooling towers for use with chilled ceilings, Applied Thermal Engineering 20 (13) (2000).

[17] TRNSYS, A Transient System Simulation Program, University of Wisconsin, Madison, USA, 1996.